Observations of Small Debris from the Cosmos 1408 Anti-Satellite Test using the HUSIR and Goldstone Radars

James Murray
Jacobs JETS Contract, NASA Johnson Space Center
Chris Ostrom
HX5 Jacobs JETS Contract, NASA Johnson Space Center
Tim Kennedy
NASA Johnson Space Center, Orbital Debris Program Office
Mark Matney
NASA Johnson Space Center, Orbital Debris Program Office

ABSTRACT

On 15 November 2021, Russia conducted a direct-ascent anti-satellite (ASAT) test against its Cosmos 1408 satellite, which had been in orbit since 1982. The test produced at least 1500 fragments trackable by the U.S. Space Surveillance Network (SSN). The test is a significant event because the resulting cloud has the potential to endanger the International Space Station and other satellites in low Earth orbit (LEO). For almost 30 years, the NASA Orbital Debris Program Office (ODPO) has used the Haystack Ultrawideband Satellite Imaging Radar (HUSIR), operated by the Massachusetts Institute of Technology's Lincoln Laboratory to perform statistical measurements of debris in LEO too small to be tracked by the SSN, nominally down to 5.5 mm at 1000 km altitude. The ODPO also utilizes the Goldstone Orbital Debris Radar (Goldstone), operated by NASA's Jet Propulsion Laboratory, to characterize the small debris environment in LEO down to approximately 3 mm at 1000 km altitude. To characterize the small debris component of the Cosmos 1408 ASAT test, a series of observation campaigns were conducted with the HUSIR and Goldstone radars. This paper discusses the observation planning, including beam overlap analysis needed for Goldstone bistatic operation, using a model of the debris cloud produced with the NASA Standard Satellite Breakup Model. A description of the radars and the data processing techniques used to analyze the data are also discussed. Finally, results of the measurement campaigns including cumulative count rate versus size and surface area flux versus altitude and inclination are presented.

1. INTRODUCTION

On 15 November 2021, Russia conducted a direct ascent anti-satellite (ASAT) test that resulted in the breakup of the Cosmos 1408 satellite. The test targeted Cosmos 1408 (International Designator 1982-092A, Catalog Number 13552), a derelict Soviet electronic and signals intelligence (ELINT) *Tselina-D*-class spacecraft. The spacecraft was launched into a 666 × 636 km altitude, 82.6-degree inclination orbit in 1982. By the time of the test, Cosmos 1408 had decayed to a 490 × 465 km altitude orbit. The test produced more than 1500 large fragments trackable by the U.S. Space Surveillance Network (SSN) immediately following the event [1]. As of 7 March 2022, 1604 fragments had been added to the U.S. Satellite Catalog. The test is a significant event because the resulting cloud has the potential to endanger the International Space Station (ISS) and other satellites in low Earth orbit (LEO).

Since the early 1990s, the NASA Orbital Debris Program Office (ODPO) has used the Haystack Ultra-Wideband Satellite Imaging Radar (HUSIR) and the Goldstone Orbital Debris Radar to characterize the population of orbital debris in LEO too small to be tracked by the SSN. HUSIR is a monostatic radar in Westford, Massachusetts (42.623287° N, 288.511846° E), which is operated by the Massachusetts Institute of Technology's Lincoln Laboratory (MIT/LL). In debris mode, the radar transmits a right-hand circularly polarized, pulsed continuous wave (CW) waveform centered at 10.1 GHz and receives both right- and left-hand circularly polarized returns, representing the orthogonal polarization (OP) and principal polarization (PP) channels, respectively, of the radar [2]. As their primary source of sub-centimeter debris data in LEO, the ODPO uses HUSIR to measure debris down to approximately 5.5 mm in size at 1000 km altitude and lower. Note that all sizes referenced herein are derived from measured radar cross-section using the radar-based NASA Size Estimation Model (SEM).

The Goldstone Orbital Debris Radar, part of the larger Goldstone Deep Space Communications Complex (GDSCC), is in the Mojave Desert near Barstow, California at 35.425901° N, 243.110462° E, and is operated by NASA's Jet Propulsion Laboratory (JPL). Goldstone transmits a linear frequency modulated (LFM) "chirp" waveform centered at 8.56 GHz and receives dual-polarization – PP and OP – returns. Goldstone supplements HUSIR measurements by extending the measurable size regime down to approximately 3 mm in size at 1000 km altitude and lower [3]. Tab. 1 summarizes and compares the debris mode operating parameters for HUSIR and Goldstone.

Tab. 1. Radar System Debris Mode Operating Parameters for HUSIR and Goldstone.

Operating Parameter	Goldstone	HUSIR
Peak Power (kW)	440	250
Transmitter Frequency (GHz)	8.56	10.10
Transmitter Wavelength (cm)	3.5	3.0
Transmitter Antenna Diameter (m)	70.0	36.6
Receiver Antenna Diameter (m)	34.0	36.6
Transmitter Half Power Beamwidth (deg)	0.03	0.058
Receiver Half Power Beamwidth (deg)	0.06	0.058
Transmitter Antenna Gain (dB)	74.24	67.23
Receiver Antenna Gain (dB)	68.42	67.23
Avg. System Temperature (K)	21.79	186
Intermediate Frequency Bandwidth (MHz)	1.5	1.25
Pulse (chirp) Duration (ms)	2.9	1.6384
Pulse (chirp) Bandwidth (kHz)	300	N/A
Pulse Repetition Frequency (Hz)	55.6	60

For orbital debris radar data collection, HUSIR operates in a "beam-park" mode in which the radar is pointed at a fixed azimuth and elevation while portions of the orbital debris environment pass through the radar beam. This observation mode simplifies the calculation of debris flux, or number of objects detected per unit area, per unit time, by providing a fixed detection volume. The primary beam-park geometry employed by HUSIR, called 75E, involves pointing at 75° elevation due East. The 75E staring geometry allows the radar to measure Doppler shift that provides meaningful orbital information – using a circular orbit approximation – while minimizing sensitivity loss due to increased atmospheric attenuation and increased free space path loss for a given altitude. In the 75E staring geometry, HUSIR samples between 392 km and 2166 km altitude.

Goldstone is a bistatic radar that uses Deep Space Station 14 (DSS-14) as a transmitter and, since 2018, DSS-25 or DSS-26 as a receiver. Due to the long baseline between transmitter and receiver, approximately 10 km, the instantaneous altitude coverage of the beam overlap is limited. This requires the transmitter and receiver to point such that the boresight of both antennas intersect at an altitude of interest. For orbital debris radar data collection, Goldstone uses a pseudo-75E observation geometry in which the transmitter is pointed at 75° elevation due East, and the receiver is pointed to intersect the transmitter beam at specific altitudes. Regular observations involve sampling between 700 km and 1000 km altitude with four different overlapping pointings.

2. OBSERVATION PLANNING

To characterize the breakup fragment cloud soon after the Russian ASAT event occurred, HUSIR and Goldstone were requested to conduct beam-park measurements focused on orbital debris beyond the SSN tracking capability. These measurements were initiated within a day of the event and conducted over several weeks to monitor the evolution of the fragment cloud. Measurements were planned at times corresponding to expected passes of the resulting debris cloud through the beam of the radar, while also accounting for the availability constraints of each sensor. A good candidate observation requires both for the cloud to pass through the beam of the radar and for the radar to be available during a time window long enough to measure a significant portion of the cloud.

To plan the special observation campaigns, a model of the debris cloud resulting from the event was generated using the NASA Standard Satellite Breakup Model (SSBM). The SSBM is described in detail in [4]. Candidate observation windows were then identified by running a two-line element set (TLE) of the Cosmos 1408 parent body

through the Satellite Trajectory and Attitude Kinetics (SATRAK) software to identify times where the satellite orbit would pass through each radar beam in their standard 75E radar geometries. The modeled cloud fragments were then propagated to the time of the candidate observation windows using the ODPO's standard long-term orbit propagator PROP3D, an orbital element propagator that includes sun-moon, J2, J3, J4, and drag perturbations. An example of the predicted range-time distribution for a candidate cloud pass on day of year (DOY) 346 is shown in Fig. 1. Although Goldstone is used in this example, the same process is used for HUSIR. The vertical red lines represent the start and stop times between which the radar, in this case Goldstone, was available for debris measurements. To evaluate whether enough of the cloud can be observed within the scheduling constraints of the radar, a cumulative count of modeled fragments passing through the beam as a function of time is generated. Fig. 2 shows one such cumulative curve, based on the cloud shown in Fig. 1, where about 93% of the cloud fragments are contained between the two red lines. Typically, the ODPO and the radar operators refine the start and stop times of candidate observations to optimize data quality within availability constraints.

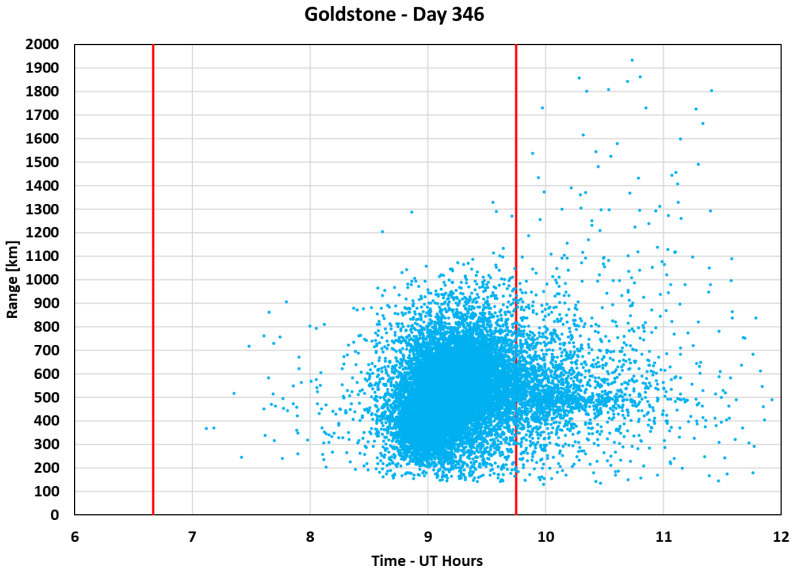

Fig. 1. Predicted range/time distribution, from the perspective of Goldstone, of Cosmos 1408 fragments for a candidate observation on DOY 346. Vertical red lines represent the start and stop times of the candidate observation.

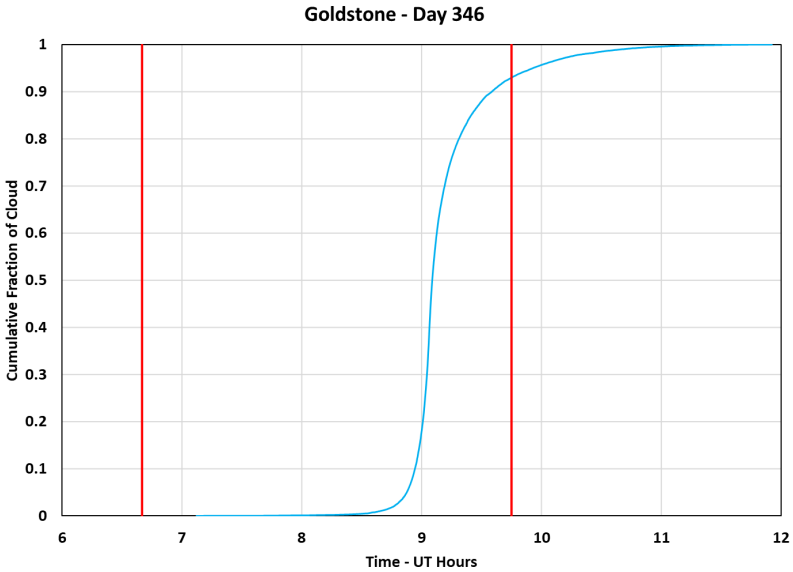

Fig. 2. Predicted cumulative fraction of the cloud as a function of time for a candidate observation on DOY 346.

Since Goldstone is a bistatic radar system, the altitude of the beam intersection must also be considered. For each candidate observation, the beam overlap as a function of range from DSS-14 was calculated for several target altitudes around the breakup altitude. The optimal pointing was that which the largest fraction of the cloud passed within the bistatic radar beam overlap. The optimal intersection altitude for the observations was approximately 472 km, close to the altitude at which the breakup is estimated to have occurred. Fig. 3 shows the normalized peak gain product of DSS-14 and DSS-25 as a function of orbit altitude illustrating the bistatic beam overlap, where the vertical, dashed black lines show the upper and lower altitude limits of the nearly 64-km-wide overlap. Details of the peak gain product calculation can be found in [3].

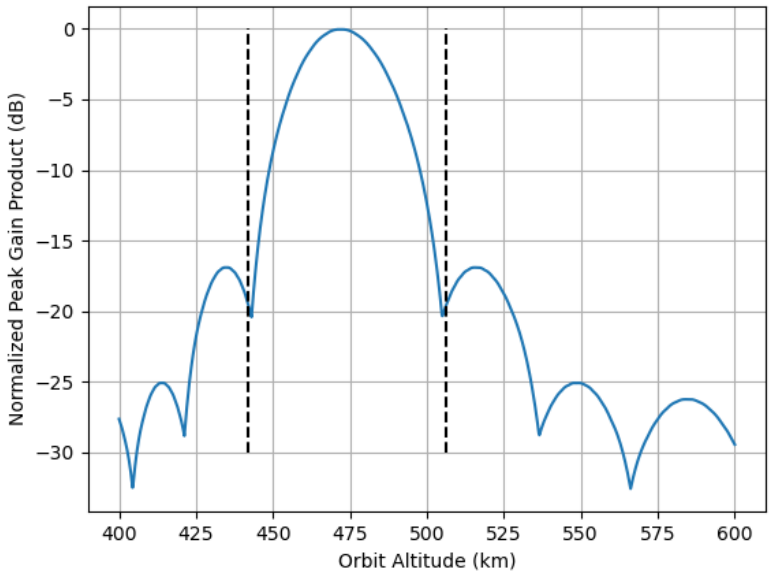

Fig. 3. Normalized peak gain product of DSS-14 and DSS-25 versus altitude illustrating the bistatic beam overlap. Vertical, dashed black lines indicate the lower and upper altitude limits of the overlap.

Fig. 4 shows the range-time distribution of a candidate observation for Goldstone on DOY 346 where the vertical red lines stand for the start and stop times of the observation and the horizontal, dashed black lines represent the bistatic beam overlap extent. The shaded region of the plot represents the subset of the range-time space to be measured by Goldstone. Including both time and altitude constraints, about 39% of the cloud would have been visible in this example. Although the bistatic nature of the radar limits its altitude coverage, Goldstone still provides unique and valuable insight into the smallest size regimes currently accessible to terrestrial radar.

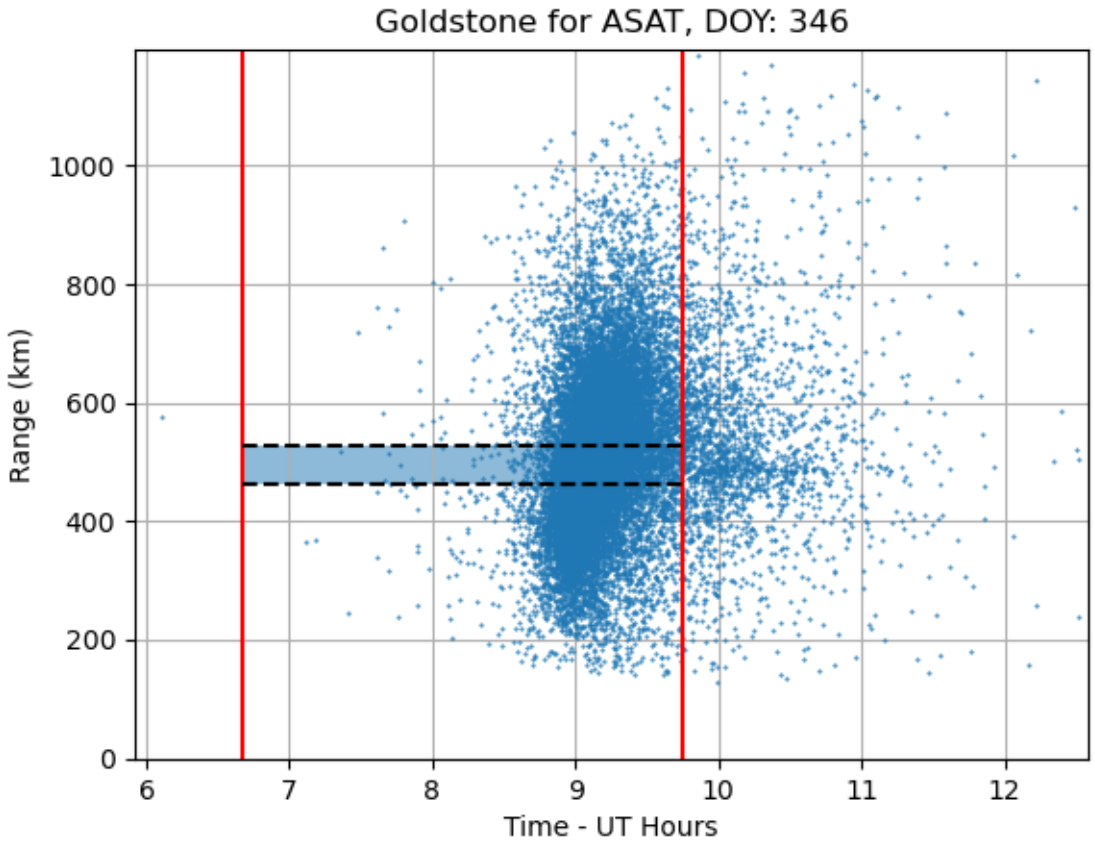

Fig. 3. Predicted range-time distribution, from the perspective of Goldstone, of Cosmos 1408 fragments for a candidate observation on DOY 346, highlighting the subset of the range/time space to be measured by Goldstone based on the bistatic beam overlap constraints.

3. REVIEW OF COLLECTED DATA AND ANALYSIS

Over a 25-day period following the ASAT test, the ODPO, with its partners at MIT/LL and JPL, conducted a radar measurement campaign successfully measuring 16 passes of the debris cloud over the course of 11 days by the 2 radars. Tab. 2 describes the dates of data collection, number of debris cloud passes, debris counts, and observation hours for the radar measurement campaign.

When performing the beam park measurements, in addition to the cloud, the debris environment background also passes through the radar's field of view. For some time after a breakup, the fragments in a debris cloud remain grouped together in similar orbit planes. As the cloud moves through the radar's field of view, it generates a unique three-dimensional time, range, and range-rate pattern, providing a means for correlating radar detections to debris clouds. Fig. 4 shows the range versus Doppler velocity, range versus DOY, and Doppler velocity versus DOY for detections measured by HUSIR on DOY 341. The modeled cloud, which also includes debris objects with sizes too small to be detected by HUSIR, is shown in gray for reference. Detections of the Cosmos 1408 fragments may be identified and distinguished from the background debris population by applying cluster analysis across measurements of range, range-rate, and time of detection.

Tab. 2. Summary of HUSIR and Goldstone Operations for Cosmos 1408 Debris Cloud Measurements.

Radar	Day of Year (DOY)	Cloud Passes	Detections	Hours
HUSIR	320	2	152	1.40
HUSIR	321	2	163	0.99
HUSIR	322	2	149	1.22
HUSIR	323	2	166	1.02
HUSIR	324	1	79	0.33
HUSIR	325	2	140	1.11
Goldstone	327	1	144	1.48
Goldstone	328	1	104	0.96
HUSIR	341	1	60	0.76
HUSIR	344	1	66	0.84
Goldstone	345	1	77	4.99

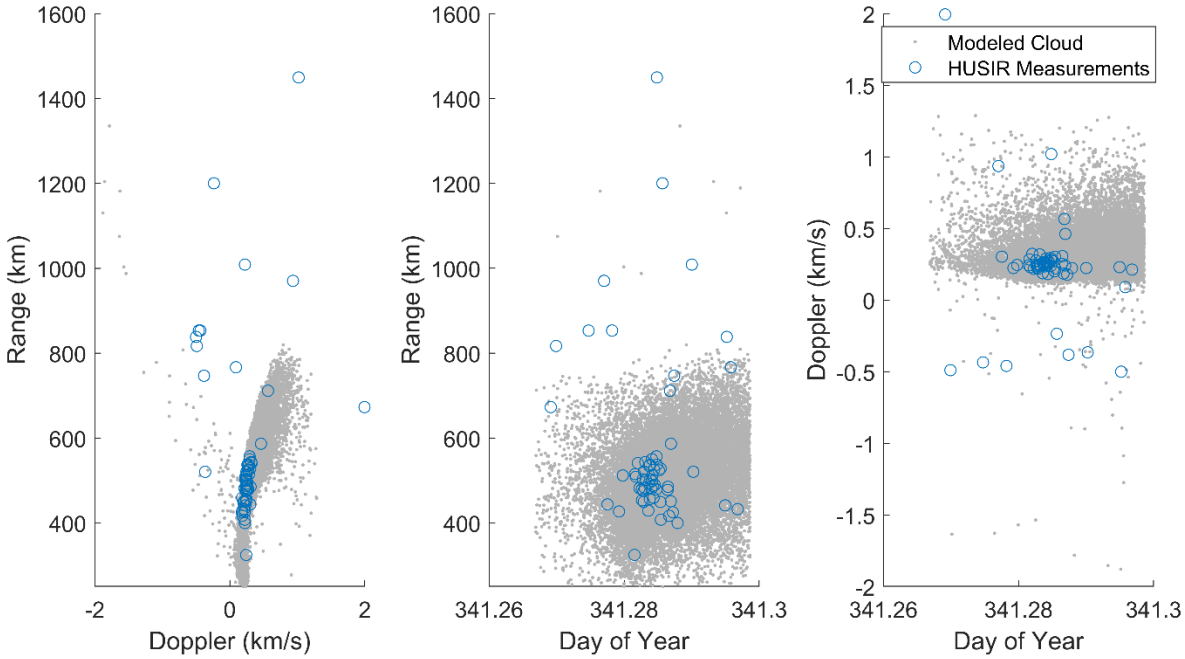

Fig. 4. Range versus Doppler velocity (left), range versus fractional DOY (middle), and Doppler velocity versus fractional DOY (right) for detections measured by HUSIR on DOY 341.

4. RESULTS

To understand the small-debris component of the Cosmos 1408 debris cloud, it is important to characterize its distribution in size, altitude, and orbital inclination, particularly as compared to the background debris population. Note that all sizes are estimated from the measured radar cross-section using the radar-based NASA SEM [5]. The cumulative count rate versus size, surface area flux versus altitude, and surface area flux versus Doppler inclination are presented, where the curves are aggregated over all observations. The results are separated by sensor since the altitude coverage and sensitivity of each sensor varies. To compare to the background population, HUSIR observations are compared to HUSIR measurements made in Calendar Year (CY) 21 before the breakup. Goldstone measurements since CY18 have focused on altitudes above 700 km [6,7]. The CY16-17 dataset is the most recent Goldstone dataset to measure below approximately 700 km altitude, so it is used for the Goldstone comparison.

Fig. 5 shows the cumulative count rate versus size of the special observations (ASAT) as compared to that of data taken by HUSIR in CY21 before the breakup. The cumulative count rate is considerably higher at all sizes smaller than 10 cm, although the overlap at sizes larger than 10 cm is likely related to the relatively low number of hours of cloud observations. Fig. 6 shows the cumulative count rate versus size of the Goldstone ASAT observations, limited to the approximate null-to-null bistatic beam overlap of the CY21 observation geometry. Like the HUSIR data, there is a significant increase in cumulative count rate over all sizes where there are enough total detections. Note that due to saturation issues, Goldstone cannot effectively measure debris larger than about a centimeter [8]. It was shown in [1] that this data, along with data from other SSN assets, matches the number of fragments predicted by the NASA SSBM very well across multiple orders of magnitude in size.

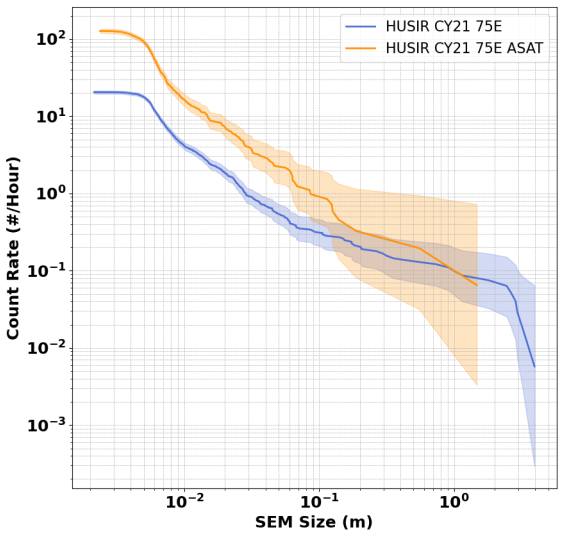

Fig. 5. Cumulative count rate of the aggregate HUSIR ASAT observations as compared to the background environment measured in CY21. The shaded regions correspond to the 2σ-Poisson confidence intervals.

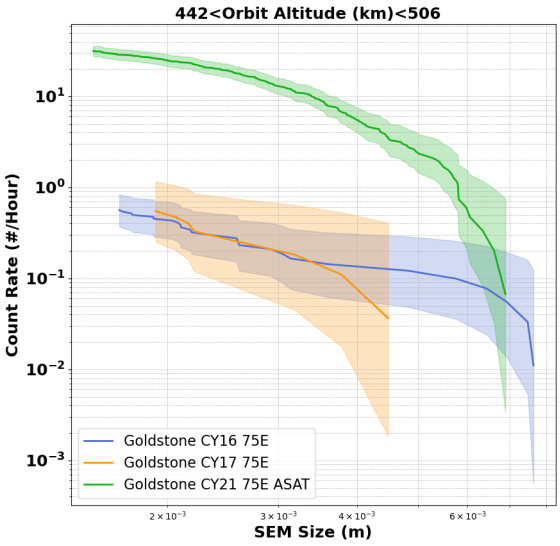

Fig. 6. Cumulative count rate of the aggregate Goldstone ASAT observations as compared to the background environment measured in CY16-17 and limited to altitudes of the main beam overlap. The shaded regions correspond to the 2σ-Poisson confidence intervals.

Fig. 7 shows the surface area flux versus altitude of the HUSIR ASAT observations compared to contemporaneous background debris environment measurements, where the flux is limited to sizes larger than 5.5 mm, the approximate size at which HUSIR measurements are complete at 1000 km altitude and lower. The highest flux occurs in the 450 km to 500 km altitude bin, corresponding to the altitude at which the breakup occurred. The flux is elevated above background levels down to the lowest altitude measurable by HUSIR in its standard debris waveform, 400 km, and up to 650 km altitude. Above 650 km, the flux measured in the special data collects was

comparable to background levels. Fig. 8 shows the surface area flux versus altitude of the Goldstone ASAT observations compared to Goldstone observations in CY16–17. The flux is limited here to sizes larger than 3 mm, the approximate size at which Goldstone measurements are complete at 1000 km altitude and lower. The vertical, dashed black lines show the approximate null-to-null bistatic beam overlap of the CY21 ASAT observation geometry. Like HUSIR, the flux peaks in the 450 km to 500 km altitude bin. It is higher than the background in adjacent bins as well, but meaningful comparisons are difficult at these altitudes, as they are effectively sidelobe detections.

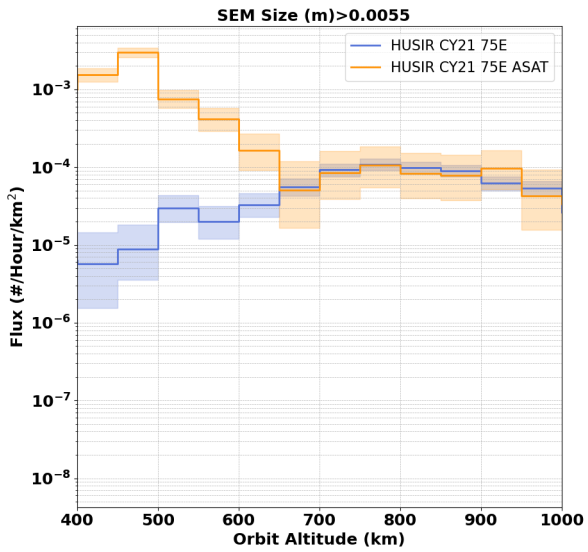

Fig. 7. Surface area flux versus altitude of the aggregate HUSIR ASAT observations as compared to the background environment measured in CY21, where flux is limited to objects 5.5 mm and larger. The shaded regions correspond to the 2σ-Poisson confidence intervals.

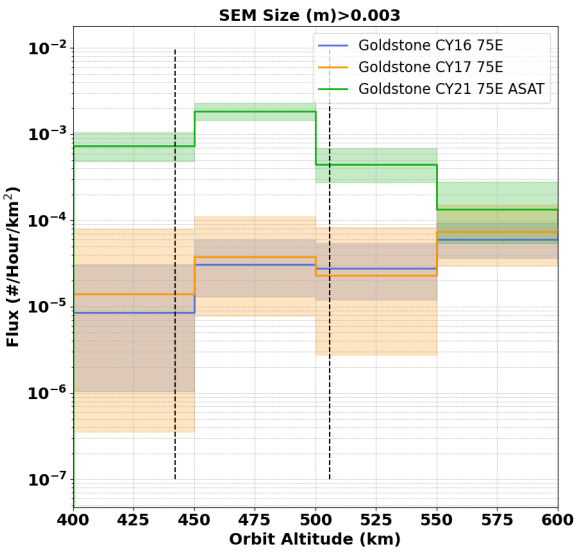

Fig. 8. Surface area flux versus altitude of the aggregate Goldstone ASAT observations as compared to the background environment measured in CY16-17, where flux is limited to objects 3 mm and larger. The vertical, dashed black lines correspond to the altitude coverage of the main beam overlap. The shaded regions correspond to the 2σ-Poisson confidence intervals.

Fig. 9 shows the surface area flux versus Doppler inclination of HUSIR ASAT measurements, compared to the background, limited to altitudes less than 1000 km and sizes larger than 5.5 mm and using 2° wide bins. Here the flux is elevated above background levels from 74° to 88° inclination, with a peak flux in the 82° to 84° inclination bin, which corresponds to the inclination of the parent body. Fig. 10 shows the surface area flux versus Doppler inclination of Goldstone ASAT measurements, compared to the CY16–17 background, limited to the altitude coverage of the main beam overlap and sizes larger than 3 mm. Here, 5°-wide bins are used to compensate for the relatively fewer counts in the restricted altitude coverage of the beam overlap. Again, the peak flux occurs in the inclination bin corresponding to the inclination of the parent body, 80° to 85°. The flux is elevated above background measurements from 75° to 85° inclination.

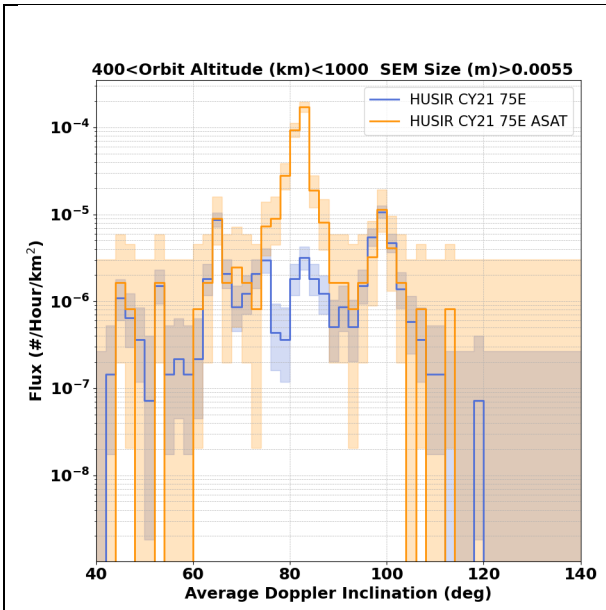

Fig. 9. Surface area flux versus Doppler inclination of the aggregate HUSIR ASAT observations as compared to the background environment measured in CY21, where flux is limited to altitudes less than 1000 km and objects 5.5 mm and larger. The shaded regions correspond to the 2σ-Poisson confidence intervals.

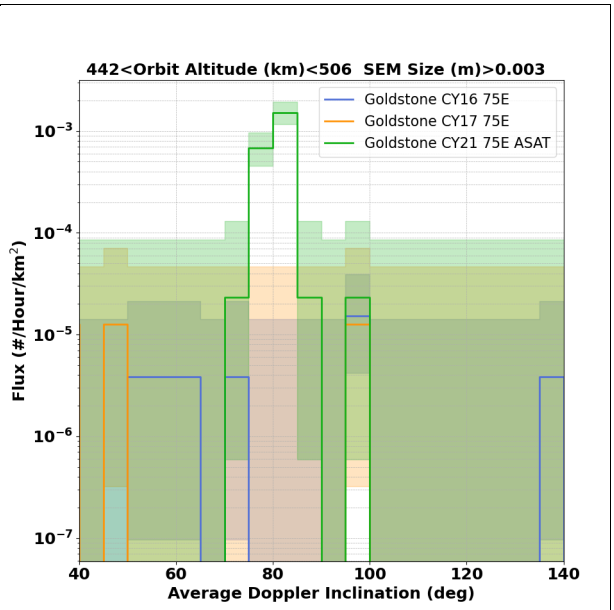

Fig. 10. Surface area flux versus altitude of the aggregate Goldstone ASAT observations as compared to the background environment measured in CY16–17, where flux is limited to objects 3 mm and larger and the altitude coverage of the main beam overlap. The shaded regions correspond to the 2σ-Poisson confidence intervals.

5. SUMMARY

The ASAT test against Cosmos 1408 on 15 November 2021 produced a significant amount of trackable (>10 cm) debris in LEO, increasing the potential collision risk with satellites and the ISS. The NASA ODPO, in partnership with MIT/LL and JPL, led a measurement campaign to characterize the debris generated by the breakup that is too small to be tracked by the SSN. Methods for observation planning were described in which the NASA SSBM was used to generate a model of the Cosmos 1408 debris cloud and fragments were propagated to observation windows identified using TLEs of the parent body. Special considerations for sensor availability and the beam overlap of the Goldstone radar were presented. Over a 25-day period following the breakup, measurements were performed with both HUSIR and Goldstone on 11 separate days resulting in 15.1 total hours of observation and 1300 total detections. It was then shown that, using the modeled debris cloud, clustering analysis could be performed to associate detections likely to be associated with the Cosmos 1408 debris cloud.

Charts of cumulative count rate versus size, surface area flux versus altitude, and surface area flux versus Doppler inclination were shown for the aggregate HUSIR and Goldstone ASAT observations, as compared to measurements of the background debris environment available from each sensor. The cumulative count rate was shown to be significantly higher than the background debris environment at all sizes for which sufficient detections were obtained. In fact, these data from HUSIR and Goldstone, as well as data from SSN assets, have been shown to match the NASA SSBM predicted number of fragments over four orders of magnitude in size. The surface area flux versus altitude for HUSIR and Goldstone ASAT observations showed a peak flux in the 450 km to 500 km altitude bin, corresponding to the altitude of the breakup. The flux was elevated above the background levels from 650 km altitude down to at least 400 km altitude, the lowest measurable by the standard HUSIR debris waveform. Surface area flux versus Doppler inclination for HUSIR and Goldstone ASAT observations showed a peak flux near the inclination of the parent body, 82° to 84° inclination. The flux was elevated above background levels from 74° to 88° inclination. This measurement campaign has shown that there is indeed a significant millimeter- and centimeter-sized debris component associated with the Cosmos 1408 ASAT test, and the analysis thereof has shown good agreement with SSBM predictions.

6. REFERENCES

[1] NASA Orbital Debris Program Office. The Intentional Destruction of Cosmos 1408, *Orbital Debris Quarterly News*, 26(1):1-5, March 2022.

[2] J. Murray and T. Kennedy. Haystack Ultra-Wideband Satellite Imaging Radar Measurements of the Orbital Debris Environment: 2020, *NASA/TP-20220006634*, May 2022.

[3] R. Miller, J. Murray, and T. Kennedy. Goldstone Radar Measurements of the Orbital Debris Environment: 2018, *NASA/TP-20210015780*, May 2021.

[4] N. Johnson, P. Krisko, J.-C. Liou, and P. Anz-Meador. NASA's new breakup model of evolve 4.0, *Advances in Space Research*, 28(9):1377-1384, 2001.

[5] Y.-l. Xu and C. Stokely. A Statistical Size Estimation Model for Haystack and HAX Radar Detections, *56th International Astronautical Congress*, Fukuoka, Japan, 2005.

[6] J. Murray. New Geometry for Debris Observations using the Goldstone Orbital Debris Radar, *Orbital Debris Quarterly News,* 23(1&2):8, 2019.

[7] C. Lee, J. Jao, M. Slade, and N. Rodriguez-Alvarez. Micro-Meteoroid and Orbital Debris Radar from Goldstone Radar Observations, *Journal of Space Safety Engineering*, 7(3):242–248, 2020.

[8] J. Murray, R. Miller, M. Matney, P. Anz-Meador, and T. Kennedy. Recent Results from the Goldstone Orbital Debris Radar: 2016-2017, *First International Orbital Debris Conference*, Sugarland, Texas, 2019.